

FRD3 Controls Iron Localization in Arabidopsis¹

Laura S. Green² and Elizabeth E. Rogers*

Departments of Biochemistry and Nutritional Sciences, University of Missouri, Columbia, Missouri 65211

The *frd3* mutant of Arabidopsis exhibits constitutive expression of its iron uptake responses and is chlorotic. These phenotypes are consistent with defects either in iron deficiency signaling or in iron translocation and localization. Here we present several experiments demonstrating that a functional *FRD3* gene is necessary for correct iron localization in both the root and shoot of Arabidopsis plants. Reciprocal grafting experiments with *frd3* and wild-type Arabidopsis plants reveal that the phenotype of a grafted plant is determined by the genotype of the root, not by the genotype of the shoot. This indicates that *FRD3* function is root-specific and points to a role for *FRD3* in delivering iron to the shoot in a usable form. When grown under certain conditions, *frd3* mutant plants overaccumulate iron in their shoot tissues. However, we demonstrate by direct measurement of iron levels in shoot protoplasts that intracellular iron levels in *frd3* are only about one-half the levels in wild type. Histochemical staining for iron reveals that *frd3* mutants accumulate high levels of ferric iron in their root vascular cylinder, the same tissues in which the *FRD3* gene is expressed. Taken together, these results clearly indicate a role for *FRD3* in iron localization in Arabidopsis. Specifically, *FRD3* is likely to function in root xylem loading of an iron chelator or other factor necessary for efficient iron uptake out of the xylem or apoplastic space and into leaf cells.

Iron is both necessary for plant growth and toxic in excess. It participates as a redox cofactor in a number of metalloenzymes involved in respiration and photosynthesis. These same redox properties allow iron to catalyze the formation of damaging oxygen radicals (Halliwell and Gutteridge, 1992). Although iron is plentiful in the earth's crust, it exists primarily in the insoluble ferric, Fe(III), form. Therefore, plants need specific mechanisms to obtain sufficient amounts of this important nutrient. Dicots rely on acidification of the rhizosphere to solubilize ferric iron, reduction of ferric iron to the more soluble ferrous form, and transport of the ferrous iron into the root epidermal cells. These activities are collectively termed iron uptake responses and are maximally expressed under conditions of iron deficiency. The genes responsible for the root iron-deficiency inducible ferric chelate reductase activity and the major ferrous uptake transporter have been identified as *FRO2* and *IRT1*, respectively, in the model plant Arabidopsis (Eide et al., 1996; Robinson et al., 1999; Vert et al., 2002).

It is well known that iron deficiency causes chlorosis in plants. On a molecular level, this chlorosis is caused by a reduction in the amount of chlorophyll synthesized and an accumulation of both Mg-protoporphyrin IX and Mg-protoporphyrin IX monomethyl ester that are chlorophyll precursors (Spiller et al., 1982). These data imply there is an iron-requiring step between Mg-protoporphyrin IX monomethyl ester and proto-

chlorophyllide (Spiller et al., 1982). Recently, CHL27 has been demonstrated to be this iron-containing protein necessary for protochlorophyllide biosynthesis in Arabidopsis (Tottey et al., 2003). CHL27 is the Arabidopsis homolog to the Chlamydomonas Crd1 protein. Both CHL27 and Crd1 are putative diiron containing enzymes and candidates for the aerobic cyclase enzyme that catalyzes the conversion of Mg-protoporphyrin IX monomethyl ester to divinyl protochlorophyllide that contains the fifth ring characteristic of all chlorophylls (Moseley et al., 2000; Tottey et al., 2003).

Relatively little is known about either the mechanisms that control the expression of iron uptake responses or those involved in iron translocation throughout the plant. Previously, we reported that the *frd3* mutant of Arabidopsis constitutively exhibits symptoms of iron deficiency (Rogers and Guerinot, 2002a). It is chlorotic, constitutively expresses its iron uptake responses, and does not accumulate the iron storage protein ferritin in its leaves, which indicates low plastid iron levels. However, when grown under certain conditions, *frd3* mutants also have higher total iron concentrations in their leaf tissue. If *frd3* is grown under conditions of high iron availability, such as petri plates containing 500 μM Fe(III)EDTA, iron accumulates in the shoots to approximately twice wild-type levels (Rogers and Guerinot, 2002a). However, if *frd3* is grown under conditions of much lower iron availability, such as standard potting soil, iron does not overaccumulate and in fact is about 10% lower than in wild-type leaves (Lahner et al., 2003). The *FRD3* gene encodes a protein predicted to be a member of the multi-drug and toxin efflux (MATE) family that is expressed only in the root. We proposed two possible roles for *FRD3*, either in iron deficiency signaling or iron localization within the plant.

¹ This work was supported by an MU Research Board grant and a USDA CSREES grant (2002-35100-12331 to E.E.R.).

² Present address: Department of Biochemistry and Molecular Biology, University of Massachusetts, Amherst, MA 01003.

* Corresponding author; e-mail rogersee@missouri.edu; fax 573-882-0185.

Article, publication date, and citation information can be found at www.plantphysiol.org/cgi/doi/10.1104/pp.104.045633.

Here we report the results of several experiments designed to distinguish between these two models for FRD3 action. First, we show that detached roots of the *frd3* mutant are capable of repressing iron uptake responses when cultured under iron-sufficient conditions. Furthermore, grafting experiments show that when *frd3* mutant shoots are appropriately supplied with iron, they regreen and the plants are capable of correctly regulating root iron uptake responses. We also show that protoplasts isolated from *frd3* mutants have lower iron levels than those from wild-type plants and that *frd3* mutant plants accumulate abnormal levels of ferric iron in their root vasculature. FRD3 is expressed in the pericycle and other vascular cylinder cells in the mature portion of the root. All of these data are consistent with a role for FRD3 in the delivery of iron to the shoot in a useable form.

RESULTS

If the wild-type FRD3 protein were involved in transmission or perception of a systemic iron deficiency signal, the loss-of-function *frd3* mutants presumably would not be able to down-regulate their iron uptake responses even though there is sufficient iron in the leaf tissues. In this signaling model, shoot chlorosis would be caused by excess iron or manganese. A signaling defect could be shoot-specific, in which case the *frd3* mutant shoot would be defective in signaling the shoot iron status to the root. Alternatively, a signaling defect could be root-specific. In this case the *frd3* mutant roots would be defective in perceiving a shoot-derived iron status signal or could not regulate their iron uptake responses as directed by the shoot-derived signal. In the other model, the FRD3 protein would be involved in iron localization. In this case, iron would not get to the leaf cells in a usable form in the *frd3* mutant, causing the shoot to be functionally iron deficient. This model is consistent with the lack of accumulation of the ferritin protein in *frd3* leaf tissue. With this model, the constitutive iron uptake responses exhibited by *frd3* mutant roots would be an appropriate response to a shoot iron deficiency signal and shoot chlorosis could be caused by iron deficiency.

Examination of Iron Status Signaling in the *frd3* Mutant

To assess the signaling capabilities of the *frd3* mutant, reciprocal grafting experiments were performed with *frd3* and wild-type seedlings. Approximately 2 weeks after grafting, plants were transferred to iron-sufficient media for 3 d, after which root ferric chelate reductase activity, and shoot chlorophyll and ferritin levels were measured (Fig. 1). Self-grafted plants behave similarly to the ungrafted controls, indicating that the grafting process itself does not affect iron homeostasis. Examining the reciprocal grafts, it is clear the phenotype of the grafted plant

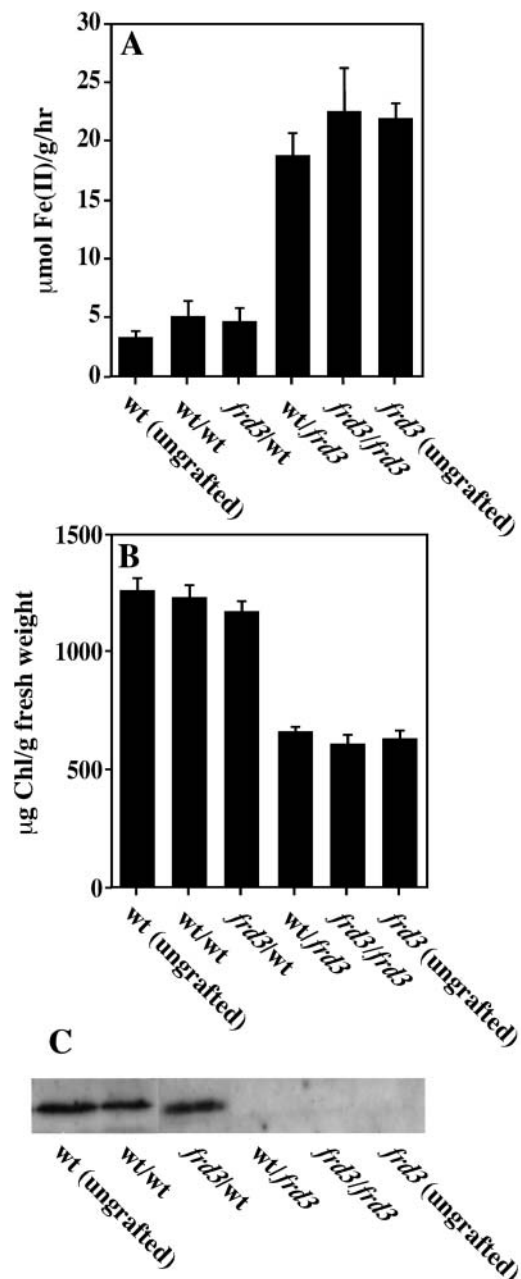


Figure 1. The *frd3* phenotype is controlled by root genotype in reciprocal grafts. Four-day-old seedlings were grafted, allowed to recover for 2 weeks, and then transferred to iron-sufficient media for 3 d. Root ferric chelate reductase activity (A) and chlorophyll content (B) were measured spectrophotometrically. Ferritin protein was measured by immunoblot using anti-ferritin antibodies (C). Labels are shoot genotype/root genotype.

follows the genotype of the root, not the genotype of the shoot. For example, when a *frd3* shoot is grafted onto a wild-type root, the *frd3* shoot is not chlorotic and accumulates the ferritin protein, and the wild-type root does not express its ferric chelate reductase activity. This indicates that the *frd3* shoot is capable of transmitting its iron sufficient status to the root and that when appropriately supplied with iron by the

wild-type root, a *frd3* shoot does accumulate chlorophyll and ferritin protein. However, when a wild-type shoot is grafted onto a *frd3* mutant root, this wild-type shoot becomes chlorotic and no longer accumulates ferritin protein, phenocopying shoots of intact *frd3* plants. This result is consistent with a model in which iron signaling is intact in the *frd3* mutant, but *frd3* roots are not capable of supplying iron to the shoots in a usable form, causing the shoots to become functionally iron deficient.

The expression of root iron uptake responses appears to be regulated by a combination of two signals, a systemic one originating in the shoot and a local one endogenous to the root (Grusak and Pezeshgi, 1996; Schikora and Schmidt, 2001). To examine local, root-endogenous signaling, we determined whether *frd3* mutant roots are capable of repressing their iron uptake responses in the absence of a shoot signal. Hypocotyls were cut and the shoot portion removed from 2-week-old seedlings that had been growing on standard media. The root portion was then transferred to either iron-sufficient or deficient media for 5 d before the roots were assayed for ferric chelate reductase activity. Measuring ferric chelate reductase activity is straightforward and was used here as a marker of all three iron deficiency responses. The absolute levels of ferric chelate reductase activity measured in the detached roots from either wild type or *frd3* are significantly lower than the reductase activity exhibited by roots of intact plants. This drop in ferric chelate reductase activity occurs immediately after shoot removal and probably reflects the nonphysiological nature of detached roots. Nevertheless, the detached roots continued to grow throughout the experiment and were able to respond to iron levels in the media (see below).

As is shown in Figure 2, wild-type detached roots behaved similarly to roots of intact wild-type plants,

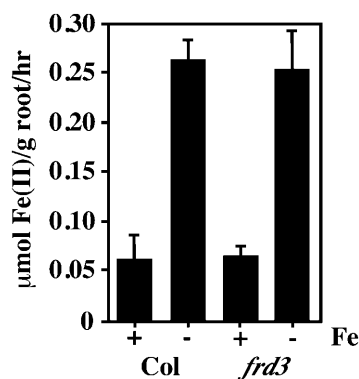


Figure 2. *frd3* mutant roots can appropriately regulate their iron deficiency responses in the absence of a shoot signal. Seedlings had the shoot portion removed prior to transfer to iron-sufficient (+Fe) or iron-deficient (−Fe) media with added Suc. The ferrozine method was used to quantitate root ferric chelate reductase 5 d after transfer. This experiment was repeated three times; a representative experiment is shown.

with ferric chelate reductase activity repressed under iron-sufficient conditions and elevated under iron deficiency. Interestingly, *frd3* mutant roots, in the absence of a shoot signal, were capable of appropriately regulating their ferric chelate reductase activity. By 5 d after transfer, the *frd3* mutant roots grown under iron-deficient conditions expressed high levels of reductase activity. More importantly, the detached *frd3* mutant roots appropriately repressed their ferric chelate reductase activity under iron-sufficient conditions, a response never seen in intact *frd3* mutant seedlings. This result is also consistent with the idea that the root mechanisms that control the iron uptake responses are functional in the *frd3* mutant, implying that the defect in the *frd3* mutant is not in its ability to down-regulate its root iron uptake responses under conditions of iron sufficiency.

Causes of Chlorosis in the *frd3* Mutant

There are two potential causes of the chlorosis observed in *frd3* mutant shoots. One is iron deficiency; that in spite of the high iron levels present in whole leaves of the *frd3* mutant, the chloroplastic or intracellular iron levels could be low. The other potential cause of chlorosis is an excess of iron or other redox active metals such as manganese (Gonzalez et al., 1998). To distinguish between these two possibilities, we determined what proportion of the iron in a plant leaf is intracellular versus apoplastic. Here, protoplasts were isolated and used as the best available assay of the intracellular fraction. Protoplasts were isolated from shoots of 2-week-old wild-type and *frd3* mutant seedlings. Previous elemental analysis on plants grown under these conditions demonstrated that *frd3* shoots contain approximately twice as much iron per gram fresh weight as do wild-type shoots (Rogers and Gueriot, 2002a). By isolating protoplasts, we removed the vascular tissue, apoplastic contents, cell walls, and any metals associated with these portions of the shoot. The protoplasts were subjected to elemental analysis and the results are shown in Figure 3. Protoplasts isolated from *frd3* mutant seedlings contain only approximately one-half as much iron on a total protein basis as do wild-type protoplasts. On the other hand, manganese levels, which are approximately 3 times higher in *frd3* shoots than in wild type, are not significantly different in protoplasts. This indicates that *frd3* chlorosis is not caused by manganese excess, since intracellular manganese levels are not increased. We have also grown *frd3* plants on manganese deficient medium and do not see a difference in either the chlorosis or constitutive ferric chelate reductase activity phenotypes of the *frd3* mutant (data not shown). The protoplast metal data indicate that extracellular or apoplastic iron and manganese must be accumulating to abnormally high levels in the *frd3* mutant. The lower intracellular iron levels in *frd3* support the hypothesis that iron is mislocalized in the *frd3* mutant.

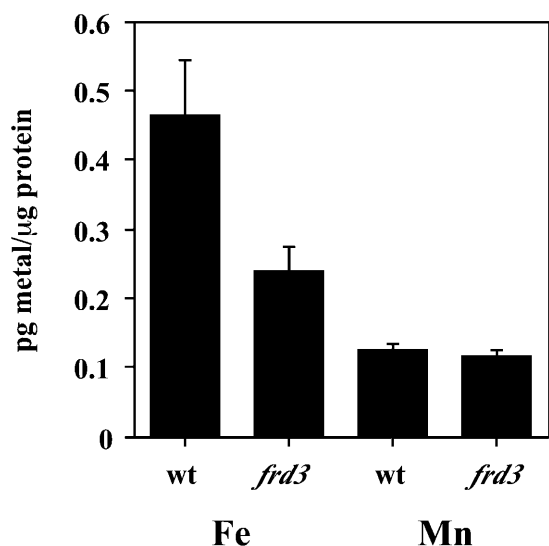


Figure 3. Protoplasts from *frd3* mutant shoots contain less iron than wild-type protoplasts. Protoplasts were isolated from 2-week-old wild-type and *frd3* protoplasts and subjected to elemental analysis. This experiment was performed three times; representative results are shown.

Iron Localization in the Root

The roots of the *frd3* mutant also accumulate excess iron (Delhaize, 1996; Rogers and Gueriot, 2002a). Since it is very difficult to obtain protoplasts from roots, we resorted to a qualitative measure of iron localization in the root tissue. Perls' stain is an acidic solution of potassium ferrocyanide, which reacts with ferric iron to form an insoluble blue precipitate. The insoluble nature of the precipitate formed in this reaction means that the blue color will not diffuse after staining and is an accurate reflection of iron localization in living tissue. As shown in Figure 4, iron accumulates to high levels in the central vascular portion of *frd3* roots. This is in contrast to wild-type roots, where iron levels throughout the root are low enough that little blue color forms with Perls' stain. Excess iron accumulation in *frd3* mutant roots is in agreement with published root iron levels in *frd3-3* (*man1*; Delhaize, 1996). Perls' staining was also performed on the leaves of wild type and *frd3* mutants; however, no staining was observed, indicating that the level of iron in the shoot vasculature of both wild type and *frd3* are below the detection limits for Perls' stain. Therefore, no conclusions about iron localization in the shoot can be drawn from this data.

Figure 4, section E shows an immunoblot of total root proteins probed with anti-ferritin antibodies. Root tissue from *frd3* mutants grown under iron-sufficient conditions shows significantly higher levels of the ferritin protein than does wild-type root tissue. This result is consistent with the higher iron levels demonstrated by elemental analysis and by Perls' stain. It also indicates that much of the iron found in *frd3* roots is

intracellular, since it triggers the accumulation of the ferritin protein.

Localization of the FRD3 Protein

We had previously reported that, by RNA blot and reverse transcription-PCR analysis, the wild-type *FRD3* gene was only expressed to detectable levels in Arabidopsis root tissue. To more precisely localize the expression of the *FRD3* gene, an FRD3-green fluorescent protein (GFP) fusion construct was used. This fusion protein is capable of complementing the *frd3-1* mutant phenotypes. Expression of the fusion protein is driven by the *FRD3* promoter to accurately reflect endogenous *FRD3* gene expression. Figure 5 shows that the *FRD3* gene is expressed in the pericycle and cells internal to the pericycle and surrounding the vascular tissue. The green fluorescence observed in the epidermis is autofluorescence; it is also present in untransformed controls and so is not due to GFP (Fig. 5, section E). The location of *FRD3* gene expression is very similar to the site of ferric iron accumulation in the *frd3* mutant.

The FRD3 protein is predicted to contain 14 transmembrane domains and to be a member of the MATE family of membrane proteins. Therefore, the FRD3 protein is predicted to localize to a membrane. Close inspection of Figure 5, section A reveals green fluorescence both internal to the pericycle cells and outlining a number of pericycle cells. While this could indicate the presence of FRD3 in the cytoplasm or on intracellular vesicles, we believe this is more likely the result of degradation of some of the FRD3-GFP fusion protein. By immunoblot, there are four protein species that cross-react with anti-GFP antibodies (data not shown). The largest of these is approximately the size of a full-length FRD3 protein fused to GFP; the other three cross-reactive bands are significantly smaller and probably represent degradation products from which some or all of the FRD3 portion of the fusion protein has been removed. For this reason, it is not possible to definitively localize the FRD3 protein on a subcellular level using this FRD3-GFP fusion protein. However, the presence of FRD3-GFP degradation products does not affect the result that the *FRD3* gene is expressed in the pericycle and vascular cylinder.

A construct containing FRD3 protein fused to the FLAG epitope tag was also constructed and transformed into wild type and the *frd3-1* mutant. By immunoblotting, there is a single anti-FLAG antibody cross-reactive species of the appropriate M_r to be the full-length FRD3-FLAG protein (data not shown). Like the FRD3-GFP fusion, the FRD3-FLAG is able to complement *frd3-1*. Immunofluorescence experiments were performed on roots expressing the FRD3-FLAG protein and showed that the FRD3-FLAG protein is present in the central vascular cylinder, the pericycle cells and smaller cells surrounding the vascular tissue (Fig. 5, section F), confirming the results obtained for the FRD3-GFP fusion.

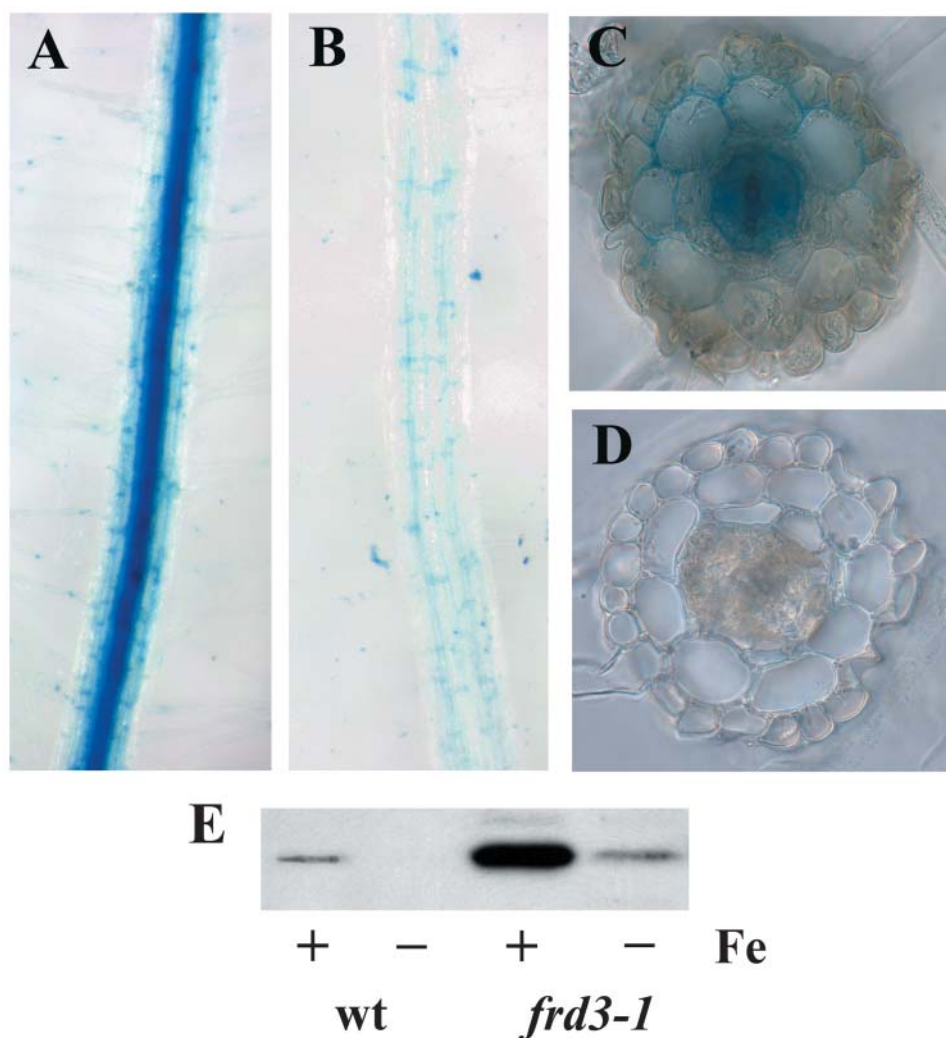


Figure 4. Iron accumulates in the vascular cylinder of *frd3* mutant roots. Five-day-old seedlings were fixed in paraformaldehyde and stained with Perl's stain to visualize ferric iron. Roots were then imbedded and 70- μ m sections cut. A, *frd3-1* intact roots; B, wild-type intact roots; C, *frd3-1* cross section; D, wild-type cross section. E, Immunoblot showing ferritin protein levels in roots of 2-week-old plants grown under iron-sufficient or deficient conditions for 3 d prior to harvest.

DISCUSSION

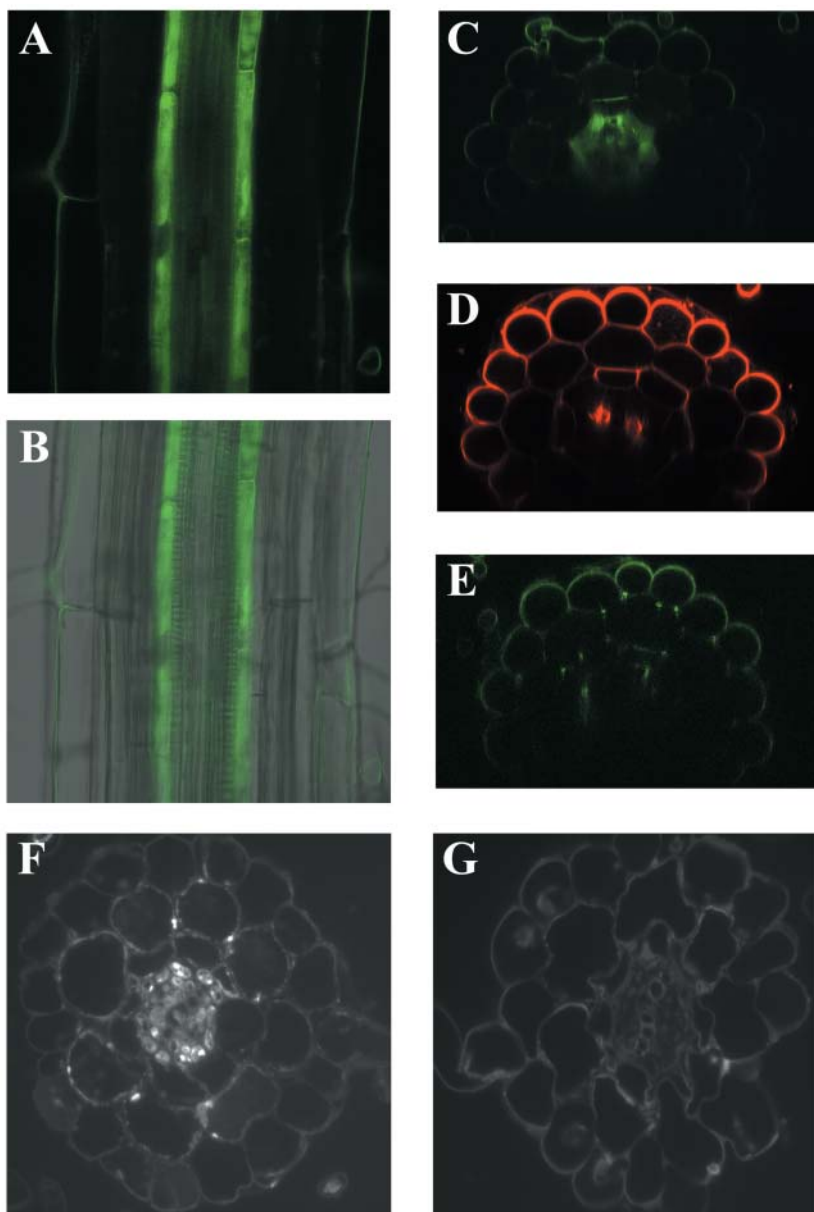
Previous work suggested two possible models of FRD3 action. The first was that FRD3 is part of an iron signaling pathway. It is likely that plant root iron uptake responses are controlled at least in part by a shoot-derived signal of shoot iron status (Grusak and Pezeshgi, 1996). This signal must both be produced by the shoot and detected in the root. If the *frd3* mutant were defective in iron signaling, the defect would likely be specific to either the shoot or the root. The reciprocal grafting experiments presented in Figure 1 indicate that the phenotype of a grafted plant is determined by the genotype of the root, not the genotype of the shoot. The fact that a wild-type root appropriately regulates its iron uptake responses when grafted to a *frd3* mutant shoot demonstrates that *frd3* mutant shoots are capable of generating a functional signal of iron status.

The competency of *frd3* mutant roots to perceive a shoot-generated signal and appropriately regulate iron uptake responses is demonstrated in the detached

root experiments presented in Figure 2. Figure 2 clearly demonstrates that in the absence of a shoot and therefore lacking a shoot-derived signal of iron status, *frd3* mutant roots appropriately regulate their ferric chelate reductase activity. This includes repressing their reductase activity when grown under iron-sufficient conditions, which is never seen in intact *frd3* mutants. These results are inconsistent with the hypothesis that the *frd3* mutant is defective in any aspect of iron deficiency signaling.

Our second hypothesis concerning FRD3 action is that FRD3 is involved in shoot iron localization. In this case, the chlorosis observed in the *frd3* would be caused by low iron levels in the shoot cells or organelles where it is needed. Here we have presented several lines of evidence that demonstrate that *frd3* mutants mislocalize iron in their tissues. Even though whole leaves of *frd3* have elevated levels of iron and manganese, *frd3* leaf protoplasts have only approximately one-half as much iron as do those from wild type (Fig. 3), and manganese levels in the two are similar. Since *frd3* shoots as a whole overaccumulate

Figure 5. *FRD3* is expressed in the root pericycle and vascular cylinder. A, Confocal fluorescence section of a root expressing FRD3-GFP fusion protein. B, GFP image from A overlaid with a transmitted light image of the same root. C, Optical cross section of a root expressing FRD3-GFP fusion protein. D, Optical cross section of a similar root stained with the cell wall dye FM-143. E, Optical cross section of a wild-type root showing epidermal autofluorescence. F, Immunofluorescence of FRD3-FLAG. G, Immunofluorescence control of a root not expressing the FLAG epitope.



both iron and manganese, two redox active metals, it was possible that the chlorosis in *frd3* shoots was caused by oxidative damage (Gonzalez et al., 1998). However, protoplasts from *frd3* contain approximately equivalent manganese levels and significantly lower iron levels, indicating that the excess metals in *frd3* mutant are spatially separated from the chloroplasts. Therefore, it is unlikely the *frd3* chlorosis is caused by metal overaccumulation. Perls' staining of wild-type and *frd3* mutant roots reveals that *frd3* roots accumulate high levels of ferric iron in the vascular cylinder (Fig. 4). This is in contrast to wild-type roots, which have much lower iron levels throughout their root tissues. Additionally, wild-type shoots grafted to *frd3* roots develop chlorosis and stop accumulating ferritin, indicating problems with iron supply and utilization.

Furthermore, *frd3* roots grafted to wild-type shoots continue to constitutively express their iron uptake responses, perhaps as a result of a signal from the iron-deficient shoot. This is strong evidence that *frd3* mutant roots cannot supply iron to the shoot in a usable form. All of the *frd3* mutant phenotypes can be explained if, in the mutant, iron is not delivered to the shoot in a form that is able to be taken up and localized appropriately in the shoot.

It is formally possible that the phenotypes of the *frd3* mutant are not caused by changes in iron uptake or localization but rather by the overaccumulation of manganese observed in *frd3* (Rogers and Guerinot, 2002a; Lahner et al., 2003). It is possible that the excess manganese in *frd3* mutants could compete with iron for uptake into leaf cells and therefore lead to iron

deficiency. However, since the intracellular manganese levels in *frd3* are no higher than they are in wild type (Fig. 3) it is unlikely that the excess manganese is successfully competing with iron for uptake either into leaf cells or into plastids. Additionally, we have grown *frd3* plants under manganese deficient conditions and see no changes in either their chlorosis or constitutive expression of root ferric chelate reductase activity (data not shown); this also argues against manganese excess causing the *frd3* mutant phenotypes. Finally, foliar application of iron tended to reduce both the leaf chlorosis and the root ferric chelate reductase activity of *frd3* mutant (data not shown). Taken together, this data strongly suggests that the *frd3* mutant phenotypes are not caused by manganese overaccumulation. Rather, we would suggest that the manganese overaccumulation is due to the constitutive expression of the IRT1 transporter, which has been shown to transport manganese (Korshunova et al., 1999).

The *FRD3* gene is expressed in the central cylinder of the root, in the pericycle cells, and cells surrounding the vascular tissues (Fig. 5). Roots of the *frd3* mutant also overaccumulate iron in this central vascular cylinder. The *FRD3* gene encodes a protein containing 14 predicted transmembrane domains. Therefore, the *FRD3* protein is likely to be associated with a cell membrane. Both the *FRD3*-GFP fusion fluorescence and the *FRD3*-FLAG immunofluorescence are brightest at the plasma membranes. However, some of the *FRD3*-GFP fusion protein is degraded and therefore cannot be used to determine subcellular localization. Additionally, cells in the central vascular cylinder are too small to be able to clearly observe plasma membrane localization. Unfortunately, the *FRD3*-FLAG protein is expressed at low levels and was not detectable by immunoelectron microscopy (data not shown). Nevertheless, the localization results presented in Figure 5 are consistent with at least some of the *FRD3* protein localizing to the plasma membrane. *FRD3* belongs to the MATE family of transmembrane proteins (Rogers and Guerinot, 2002a). Other members of the MATE family have been implicated in the efflux of low M_r organic compounds (Morita et al., 1998, 2000).

Together with the data presented, this leads to a new question: how can a putative effluxer of low M_r compounds that is expressed around the root vasculature affect iron localization in the shoot? Iron reaches the shoot tissue in sufficient amounts in the *frd3* mutant; even in soil-grown *frd3* shoots, shoots grown under conditions of low iron availability, iron levels are only about 10% lower than in wild type (Lahner et al., 2003). This is consistent with iron being loaded into the xylem appropriately in the *frd3* mutant since significant amounts of iron do reach the shoot; we do not believe that the *FRD3* protein is directly responsible for iron loading into the xylem or for other iron transport steps. The problem in the *frd3* mutant appears to be getting iron out of the xylem and into the shoot symplast and then to the chloroplasts. However, since *FRD3* is not expressed to detectable

levels in the shoots, it is doubtful that *FRD3* acts in the shoots, either as an iron transporter or otherwise. This is also consistent with the reciprocal grafting experiments that indicate *FRD3* is not needed in the shoots for wild-type iron localization and signaling.

Given *FRD3*'s expression in cells surrounding the root vasculature, we hypothesize that *FRD3* effluxes into the xylem a low M_r compound that is necessary for correct iron unloading from the xylem in the shoot. This compound could be an iron chelator. Certainly, given the low solubility of ferric iron at the pH of the xylem, approximately pH 6, ferric iron would need to be chelated to move efficiently. It is widely thought that iron moves in the xylem as ferric citrate (Pich et al., 1994; von Wirén et al., 1999). Although the *FRD3* protein could be a citrate transporter, it does not share sequence similarity to other known citrate effluxers. Nicotianamine (NA) is another molecule that has been implicated in long distance iron transport in plants. From gene expression studies of both the *chloronerva* (*chl*n) gene in tomato and the nicotianamine synthase genes in Arabidopsis, it appears that NA is synthesized throughout the plant (Ling et al., 1999; Suzuki et al., 1999). It is not known where, or via what type of transporter, NA is loaded into the vasculature; this is a possible function for *FRD3*. However, because the NA-less *chl*n mutant has alterations in copper homeostasis as well as in iron homeostasis (Pich et al., 1994; Herbig et al., 1996) and the *frd3* mutant does not have alterations in copper levels (Lahner et al., 2003), it is unlikely that the *frd3* mutant has defects in NA metabolism and transport or that the *FRD3* protein is involved in NA transport.

The *FRD3* protein also could transport one of a variety of compounds necessary for iron uptake in the shoot. Once the ferric iron reaches the shoot apoplast, it is thought to be reduced, probably by a member of the FRO (ferric reductase oxidase) family. *FRD3*'s substrate could be involved in presenting iron to the reductase. After reduction, the ferrous iron could be transported inside the leaf cells either on its own, perhaps by a member of the ZIP (Zrt-Irt-like protein) family (Rogers and Guerinot, 2002b), or as a complex with NA, via one of the YSL (yellow-stripe like) family of transporters (Curie et al., 2001; DiDonato et al., 2003). A number of yellow-stripe like genes are expressed in the shoots and may be responsible for unloading iron from the xylem. It is also possible that *FRD3* effluxes a molecule necessary for maintaining pH in the xylem. If the xylem pH was slightly higher in the *frd3* mutant than in wild type, that could lower iron solubility in the xylem just enough to cause the observed difficulty in shoot iron uptake. However, the pH of xylem fluid exuded from cut hypocotyls of *frd3* mutant plants is approximately 5.5, a little lower than xylem fluid from wild type, which is approximately 5.8 (T.P. Durrett and E.E. Rogers, unpublished data). The xylem pH of iron deficient plants can be lower than that of iron sufficient plants (Lopez-Millan et al., 2000). Therefore, the observed xylem pH difference

may simply be caused by *frd3*'s constitutive iron deficiency rather than a defect in xylem loading in the *frd3* mutant. The xylem pH difference between wild type and *frd3* might affect which ligands preferentially bind iron in the xylem but it would not be expected to reduce iron solubility in the *frd3* xylem. Although further work will be required to identify the substrate of FRD3, we can predict that it would have certain characteristics: it will be necessary for iron reduction in or unloading from the xylem or shoot apoplast, and it will have to be loaded into the xylem in the root.

MATERIALS AND METHODS

Arabidopsis Lines and Growth Conditions

The Arabidopsis mutants *frd3-1* and *frd3-3* and the corresponding wild type Columbia *gl-1* have been described previously (Rogers and Guerinot, 2002a). Plants were grown under constant 150 $\mu\text{mol photons/m}^2/\text{s}$ light at 22°C and under sterile conditions as previously described (Rogers and Guerinot, 2002a), except for the detached root experiments and seedling timecourse where 20 g/L Suc was added to the iron sufficient and iron deficient media (Yi and Guerinot, 1996). Ferric chelate reductase assays also were described previously (Yi and Guerinot, 1996).

Reciprocal Grafting

Micrografting of Arabidopsis seedlings was performed as described (Turnbull et al., 2002). Single-hypocotyl 90° butt grafts were performed on 4- or 5-d-old seedlings; collars were not used. Grafted plants were allowed to recover for 5 d at 26°C and constant 150 $\mu\text{mol photons/m}^2/\text{s}$ light. Graft integrity was verified by physical strength of the graft site, an absence of adventitious roots on the scion and robust growth of the both the root system and scion.

Detached Root Experiments

Arabidopsis seedlings were grown on Gamborg's B5 medium (Caisson Labs, Sugar City, ID) for approximately 2 weeks. The hypocotyl was cut with a sharp razor blade and shoot was removed. The root was immediately transferred to iron sufficient or iron deficient media prepared as described except for the addition of 20 g/L Suc. After 5 d, ferric chelate reductase activity was assayed as described (Yi and Guerinot, 1996). Under these conditions, the detached roots continued to grow and did not become necrotic in appearance.

Chlorophyll Extraction and Quantitation

Chlorophyll was extracted in methanol and absorbance measured at 652, 665, and 750 nm. Total chlorophyll concentration was calculated as described (Porra et al., 1989).

Immunoblots

Immunoblots were performed as previously described (Connolly et al., 2002). Total protein was prepared from the roots and shoots of plants grown axenically on plates that were either iron-deficient or iron-sufficient. Extracts were prepared by grinding tissue (1–2 mL buffer/1 g wet tissue) on ice in extraction buffer (50 mM Tris, pH 8.0, 5% glycerol, 4% SDS, 1% polyvinylpyrrolidone, 1 mM phenylmethylsulfonyl fluoride), followed by centrifugation at 4°C for 15 min at 14,000g. The supernatant was recovered and total protein was estimated using the BCA protein assay (Pierce, Rockford, IL). Samples for SDS-PAGE were diluted with an equal volume of 2× sample prep buffer (Ausubel et al., 2004) and boiled for 2 min.

Total protein (10 μg) was separated by SDS-PAGE (Laemmli, 1970) and transferred to nitrocellulose membrane by electroblotting (Towbin et al., 1979). Equal loading of blot lanes was verified by Coomassie staining of equivalently loaded gels run in parallel (Ausubel et al., 2004). Membranes were blocked in

1× PBST (0.1% Tween 20 in 1× PBS) with 5% nonfat dry milk for 3 h at 37°C and then washed 2 times in 1× PBST for 5 min each. The membranes were then incubated overnight at 4°C an anti-ferritin antibody (1:1,000-fold dilution in 1× PBST, 1% nonfat dry milk). The ferritin antibody was raised against purified pea seed ferritin (Van Wuytswinkel et al., 1995) and was the kind gift of Dr. Jean-François Briat. It has previously been shown to cross react with Arabidopsis ferritin (Gaymard et al., 1996). Next, the membranes were washed in 1× PBST, four times for 15 min each. Membranes were then incubated for 1 h with goat-anti-rabbit IgG conjugated to Horseradish peroxidase (1:5,000 dilution in 1× PBST, 1% nonfat dry milk; Pierce) followed by 4 washes for 15 min each in 1× PBST. Chemiluminescence was performed using the SuperSignal West Pico chemiluminescent substrate kit (Pierce).

Protoplast Isolation and Elemental Analysis

Arabidopsis protoplasts were isolated as previously described (Fitzpatrick and Keegstra, 2001). Protoplast integrity was verified by microscopic examination. Total protoplast protein levels were measured with a BCA Protein Assay Kit (Pierce). Iron and manganese levels were measured at the MU Research Reactor Center in a VG AXIOM high resolution ion coupled plasma mass spectrometry (ICP-MS).

Perls' Stain for Ferric Iron

Arabidopsis roots were treated with Perls' stain according to established histological methods for mammalian tissues. Briefly, equal amounts of solutions of 4% (v/v) HCl and 4% (w/v) potassium ferrocyanide were mixed immediately prior to use. The stain solution was vacuum infiltrated into 6- or 7-d-old Arabidopsis seedlings for approximately 15 min. Seedlings were rinsed in water and Perls' staining was observed immediately in whole roots. For cross-sections, after staining seedlings were fixed in 4% (w/v) paraformaldehyde and imbedded in 4% (w/v) low-melt agarose. Approximately 70- μm sections were cut with a Lancer series 1000 Vibratome (Vibratome, St. Louis).

FRD3-Fusion Constructs and Localization

The *FRD3* genomic sequence cloned into pCambia2300 has been previously described (Rogers and Guerinot, 2002a). A convenient restriction site at the 3' end of the *FRD3* coding sequence in this construct was used to insert DNA coding for the desired fusion. For the *FRD3-GFP* construct, the *GFP* gene sequence was obtained by PCR from a version optimized for plant expression (Davis and Vierstra, 1998). For the *FRD3-FLAG* construct, the FLAG sequence (DYKDDDDK) was encoded in custom synthesized oligonucleotides that were phosphorylated, hybridized to each other, and ligated into the cut *FRD3* genomic sequence. All molecular biology techniques were performed using standard protocols (Ausubel et al., 2004). The fusion clones were introduced into wild-type and *frd3-1* Arabidopsis by *Agrobacterium tumefaciens*-mediated transformation (Clough and Bent, 1998). At least six independent transformants of each construct in the *frd3-1* mutant were examined to confirm complementation by the *FRD3*-fusion constructs. With each construct in wild-type Columbia *gl-1* Arabidopsis, 8 to 10 independent lines were analyzed by segregation to confirm a single insertion event and obtain lines homozygous for the insertion. Preliminary localization was performed on 5 independent *FRD3-GFP* lines and 2 independent *FRD3-FLAG* lines. For each, one representative line was chosen for detailed analysis.

GFP fluorescence was visualized in living whole-mount roots using a Bio-Rad (Hercules, CA) Radiance 2000 confocal system coupled to an Olympus IX70 inverted microscope at the University of Missouri Molecular Cytology Core facility. Roots from *FRD3-FLAG* transgenics were fixed, embedded in methacrylate, sectioned, and stained for immunofluorescence as previously described (Baskin and Wilson, 1997).

Upon request, all novel materials described in this publication will be made available in a timely manner for noncommercial research purposes.

ACKNOWLEDGMENTS

The authors thank Tobias Baskin and Jan Judy-March for help with microscopy and immunofluorescence, Amanda Crawford and Dave Robertson for the ICP-MS analysis, Fritz Bienfait for helpful suggestions, and David Eide, Dirk Charlson, and Mary Lou Guerinot for critical reading of the manuscript.

Received April 30, 2004; returned for revision May 25, 2004; accepted May 30, 2004.

LITERATURE CITED

- Ausubel FM, Brent R, Kingston RE, Moore DD, Seidman JG, Smith JA, Struhl K (2004) Current Protocols in Molecular Biology. John Wiley & Sons, New York
- Baskin TI, Wilson JE (1997) Inhibitors of protein kinases and phosphatases alter root morphology and disorganize cortical microtubules. *Plant Physiol* **113**: 493–502
- Clough SJ, Bent AF (1998) Floral dip: a simplified method for *Agrobacterium*-mediated transformation of *Arabidopsis thaliana*. *Plant J* **16**: 735–743
- Connolly EC, Fett J, Guerinot ML (2002) Transgenic plants engineered to overexpress the IRT1 metal transporter reveal post-transcriptional regulation by metals. *Plant Cell* **14**: 1347–1357
- Curie C, Panaviene Z, Loulergue C, Dellaporta SL, Briat J-F, Walker EL (2001) Maize *yellow stripe1* encodes a membrane protein directly involved in Fe(III) uptake. *Nature* **409**: 346–349
- Davis SJ, Vierstra RD (1998) Soluble, highly fluorescent variants of green fluorescent protein (GFP) for use in higher plants. *Plant Mol Biol* **36**: 521–528
- Delhaize E (1996) A metal-accumulator mutant of *Arabidopsis thaliana*. *Plant Physiol* **111**: 849–855
- DiDonato R, Roberts L, Pierson A, Walker E (2003) The Arabidopsis yellow-stripe1-like (YSL) family of metal-nicotianamine transporters. In 1st Pan-American Plant Membrane Biology Workshop, Cuernavaca, Mexico, International Center for Genetic Engineering and Biotechnology
- Eide D, Broderius M, Fett J, Guerinot ML (1996) A novel iron-regulated metal transporter from plants identified by functional expression in yeast. *Proc Natl Acad Sci USA* **93**: 5624–5628
- Fitzpatrick L, Keegstra K (2001) A method for isolating a high yield of Arabidopsis chloroplasts capable of efficient import of precursor proteins. *Plant J* **27**: 59–65
- Gaymard E, Boucherez J, Briat JF (1996) Characterization of ferritin mRNA from *Arabidopsis thaliana* accumulated in response to iron through an oxidative pathway independent of abscisic acid. *Biochem J* **318**: 67–73
- Gonzalez A, Steffen KL, Lynch JP (1998) Light and excess manganese. Implications for oxidative stress in common bean. *Plant Physiol* **118**: 493–504
- Grusak MA, Pezeshgi S (1996) Shoot-to-root signal transmission regulates root Fe(III) reductase activity in the *dgl* mutant of pea. *Plant Physiol* **110**: 329–334
- Halliwell B, Gutteridge JMC (1992) Biologically relevant metal ion-dependent hydroxyl radical generation. *FEBS Lett* **307**: 108–112
- Herbik A, Giritch A, Horstmann C, Becker R, Balzer H, Bäumlein H, Stephan UW (1996) Iron and copper nutrition-dependent changes in protein expression in a tomato wild type and the nicotianamine-free mutant *chloronerva*. *Plant Physiol* **111**: 533–540
- Korshunova Y, Eide D, Clark G, Guerinot M, Pakrasi H (1999) The Irt1 protein from *Arabidopsis thaliana* is a metal transporter with broad specificity. *Plant Mol Biol* **40**: 37–44
- Laemmli UK (1970) Cleavage of structural proteins during the assembly of the head of bacteriophage T4. *Nature* **227**: 680–685
- Lahner B, Gong J, Mahmoudian M, Smith E, Abid K, Rogers E, Guerinot M, Harper J, Ward J, McIntyre L, et al (2003) Ionomics: The genomic scale profiling of nutrient and trace elements in *Arabidopsis thaliana*. *Nat Biotechnol* **21**: 1215–1221
- Ling H-Q, Koch G, Baumlein H, Ganai MW (1999) Map-based cloning of *chloronerva*, a gene involved in iron uptake of higher plants encoding nicotianamine synthase. *Proc Natl Acad Sci USA* **96**: 7098–7103
- Lopez-Millan AE, Morales F, Abadia A, Abadia J (2000) Effects of iron deficiency on the composition of the leaf apoplastic fluid and xylem sap in sugar beet. Implications for iron and carbon transport. *Plant Physiol* **124**: 873–884
- Morita Y, Kataoka A, Shiota S, Mizushima T, Tsuchiya T (2000) NorM of *Vibrio parahaemolyticus* is a Na⁺-driven multidrug efflux pump. *J Bacteriol* **182**: 6694–6697
- Morita Y, Kodama K, Shiota S, Mine T, Kataoka A, Mizushima T, Tsuchiya T (1998) NorM, a putative multidrug efflux protein, of *Vibrio parahaemolyticus* and its homolog in *Escherichia coli*. *Antimicrob Agents Chemother* **42**: 1778–1782
- Moseley J, Quinn J, Eriksson M, Merchant S (2000) The *Crd1* gene encodes a putative di-iron enzyme required for photosystem I accumulation in copper deficiency and hypoxia in *Chlamydomonas reinhardtii*. *EMBO J* **19**: 2139–2151
- Pich A, Scholz G, Stephan UW (1994) Iron-dependent changes of heavy metals, nicotianamine, and citrate in different plant organs and in the xylem exudate of two tomato genotypes. Nicotianamine as possible copper translocator. *Plant Soil* **165**: 189–196
- Porra R, Thompson W, Kreidemann P (1989) Determination of accurate extinction coefficients and simultaneous equations for assaying chlorophylls a and b extracted with four different solvents: verification of the concentration of chlorophyll standards by atomic absorption spectroscopy. *Biochim Biophys Acta* **975**: 348–394
- Robinson NJ, Procter CM, Connolly EL, Guerinot ML (1999) A ferric-chelate reductase for iron uptake from soils. *Nature* **397**: 694–697
- Rogers EE, Guerinot ML (2002a) FRD3, a member of the multidrug and toxin efflux family, controls iron deficiency responses in Arabidopsis. *Plant Cell* **14**: 1787–1799
- Rogers EE, Guerinot ML (2002b) Iron Acquisition in Plants. In D Templeton, ed, Molecular and Cellular Iron Transport. Marcel Dekker, New York, pp 359–373
- Schikora A, Schmidt W (2001) Iron stress-induced changes in root epidermal cell fate are regulated independently from physiological responses to low iron availability. *Plant Physiol* **125**: 1679–1687
- Spiller S, Castelfranco A, Castelfranco P (1982) Effects of iron and oxygen on chlorophyll biosynthesis. 1. *In vivo* observations on iron and oxygen-deficient plants. *Plant Physiol* **69**: 107–111
- Suzuki K, Higuchi K, Nakanishi H, Nishizawa NK, Mori S (1999) Cloning of nicotianamine synthase genes from *Arabidopsis thaliana*. *Soil Sci Plant Nutr* **45**: 993–1002
- Totter S, Block M, Allen M, Westergren T, Albrieux C, Scheller H, Merchant S, Jensen P (2003) Arabidopsis CHL27, located in both envelope and thylakoid membranes, is required for the synthesis of protochlorophyllide. *Proc Natl Acad Sci USA* **100**: 16119–16124
- Towbin H, Staehelin T, Gordon J (1979) Electrophoretic transfer of proteins from polyacrylamide gels to nitrocellulose sheets: procedure and some applications. *Proc Natl Acad Sci USA* **76**: 4350–4354
- Turnbull C, Booker J, Leyser H (2002) Micrografting techniques for testing long-distance signalling in Arabidopsis. *Plant J* **32**: 255–262
- Van Wuytswinkel O, Savino G, Briat J-F (1995) Purification and characterization of recombinant pea-seed ferritins expressed in *Escherichia coli*: influence of N-terminus deletions on protein solubility and core formation in vitro. *Biochem J* **305**: 253–261
- Vert G, Grotz N, Dédaldéchamp F, Gaymard E, Guerinot M, Briat J-F, Curie C (2002) IRT1, an Arabidopsis Transporter Essential for Iron Uptake from the Soil and Plant Growth. *Plant Cell* **14**: 1223–1233
- von Wirén N, Klair S, Bansal S, Briat J-F, Khodr H, Shioiri T, Leigh RA, Hider RC (1999) Nicotianamine chelates both Fe(III) and Fe(II). Implications for metal transport in plants. *Plant Physiol* **119**: 1107–1114
- Yi Y, Guerinot ML (1996) Genetic evidence that induction of root Fe(III) chelate reductase activity is necessary for iron uptake under iron deficiency. *Plant J* **10**: 835–844